The bio-inspired chaotic robot

Iñaki Rañó

Abstract— Chaos is an interesting phenomenon displayed by non-linear systems that has been used in robotics and found empirically on real robots' behaviour. This paper presents a formal proof that Braitenberg vehicle 2b, a bio-inspired control mechanism for unicycle robots, behaves as a mass in a potential well. This provides a powerful analogy to understand Braitenberg vehicle 2b as a mechanical system and it implies that its behaviour can be chaotic. Implementing a Braitenberg vehicle in robotics entails defining a stimulus function in the environment. Inspired by previous works and using the obtained theoretical results, this paper proposes the free area perceived by a robot as a stimulus to generate collision free continuous chaotic motion on a bounded space. In non-linear systems chaos appears when a parameter is changed in a family of dynamical systems. Similarly, our implementation on a real robot demonstrates that both, chaotic and non chaotic trajectories can be obtained depending on the stimulus function built. The behaviour is explained through the analogy with the mass in the potential well.

I. INTRODUCTION

Chaos is an interesting phenomenon displayed by non-linear dynamical systems, but is not thought as a positive feature since it involves instability and lack of long term predictability. Sometimes it is even mistaken by randomness but, contrary to randomness, chaotic behaviour can be predicted and shows properties that have been exploited for cryptography [1] or communications [2], and many other applications are investigated under the general area of control of chaos [3].

Chaos has been used in robotics too as a technique for coverage, since the trajectories generated by chaotic systems are dense. This means that the robot trajectory will pass arbitrarily close to any point in the state space. In [4] the Arnold equation, a chaotic system found in fluid dynamics, is used to control a wheeled robot to cover a work-space using for the first time chaos in robotics. They demonstrate and justify how their chaotic controller outperforms random based control for coverage. A different approach is used in [5] for a patrolling task, where a chaotic system is used to generate random points for a planner. They achieve fast coverage, but in this case chaos is just used as a random number generator. In an empirical work [6], evidences of chaos have been identified in the behaviour of a wheeled robot by computing the correlation dimension of the perceptual signals of the robot. Other experimental works [7] [8] identified positive values for the Lyapunov exponents in the trajectory described by a mobile robot, which can be clearly interpreted as deterministic chaos. Despite these findings, to the best knowledge of the author, no theoretical work shows

chaos appears on mobile robots under a deterministic control mechanism. In this paper, we show that a bio-inspired controller, a Braitenberg vehicle, can generate chaotic behaviour on a mobile robot.

Braitenberg vehicles are qualitative models of animal tropotaxis behaviour [9] and have been used for decades in robotics on an empirical basis. According to the thought experiment presented in [10], each vehicle displays a different behaviour. This paper focuses on Braitenberg vehicle 2b, which consists on a dual-drive wheeled vehicle with two sensors symmetrically arranged as shown in Figure 1. The vehicle is immersed in a stimulus field. Each sensor is linked through an increasing connection (represented on the figure by the the '+' sign) to the motor on the opposite side. Since the connection between the sensors and the motors is increasing, the more intense the stimulus gets the faster the opposite wheel turns. The overall effect is to make the robot turn towards high values of the stimulus and to speed up. In the original work [10], this behaviour is called aggression since, for a stimulus source, the vehicle acts like trying to hit the source, but in biological terms is just a taxis model.
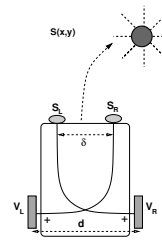

Fig. 1.   Internal structure of the Braitenberg vehicle 2*b*.

Multiple applications of this vehicle can be found in the literature providing robots with different abilities. Obstacle avoidance and target acquisition are achieved in [11] using Braitenberg vehicle 2b and 3a respectively. Vehicle 2b is used with infra-red sensors and 3a with light sensors to implement phototaxis. Braitenberg vehicles are also used in [12] for local navigation, where vehicle 2b is used for goal seeking, and vehicles 3b and 2a are used to avoid obstacles in the front and back of the robot respectively. This Braitenberg control system uses a set of fuzzy rules that generate an offset velocity for each wheel instead of the velocity itself. The first underwater robotic implementation of rheotaxis is presented in [13], where a fish robot provided with pressure sensors can keep its orientation relative to a laminar flow. Even though the forward speed is kept fixed, the turning rate of the robotic fish is computed following the principles

Iñaki Rañó is with the Intelligent Systems Research Centre, University of Ulster, UK. i.rano@ulster.ac.uk

of Braitenberg vehicles. This is not the only application of these vehicles to underwater robotics, since a robotic electric fish using a similar approach is presented in [14]. In this case the steering control is performed using the difference between the currents, perceived through electrodes, on the sides of the robot. The resulting trajectories approach conductive objects in a pond while avoiding isolating ones. As we have seen, Braitenberg vehicles are widely used to implement bio-inspired robotic behaviours, specially when the motion relies on unconventional sensors, sensors not providing distance readings. Other types of these vehicles are used in the literature to implement target seeking or avoidance behaviours, but in this review we focused on 2b type.

The main contribution of this paper is to present a proof that the controller implemented by Braitenberg vehicle 2b can show chaotic behaviour In nature chaos is the norm rather than the exception [15]. The same occurs for the controller presented in this paper. Despite non chaotic dynamics can be found, it is restricted to a set of simple conditions. On the other hand, chaotic behaviour generates dense trajectories, which makes this mechanism suitable for a wide range of applications like coverage, surveillance or exploration. Therefore, a second contribution of this paper, relevant to robotics, is the implication that these vehicles can be used for such applications. Probably the most advantageous feature of the presented controller is its simplicity of implementation, since it is based on sensorial readings from any proximity sensor. Finally, our last contribution is the design, implementation and test on a real robot of a Braitenberg controller which ensures collision avoidance with obstacles while continuously moving. The rest of the paper is organised as follows. Section II reviews the mathematical model of the vehicle and shows some mathematical properties of their trajectories, and its equivalence to a mass in a potential well. Section III proposes a novel way of implementing the Braitenberg vehicle 2b on a robot with standard range sensors and shows how experimental results match the theory. The paper ends with some conclusions and guidelines for further work in Section IV.

II. A CHAOTIC BRAITENBERG VEHICLE CONTROLLER

A. The Braitenberg vehicle 2b controller

This section states our working assumptions and reviews the controller of Braitenberg vehicle 2b (see [16] for a complete derivation of the mathematical equations). We will assume a scalar stimulus or potential $S(\mathbf{x})$ exists in a simply connected and compact (closed and bounded) set as shown in figure 2. For convenience we will separate its interior and its boundary $D \cup \partial D \in \Re^2$, where ∂D could represent the boundaries of the workspace and the obstacles. Without loss of generality, we will assume the boundary ∂D defines the limit of the influence of the stimulus, i.e. $S(\mathbf{x}) = 0$ for all $\mathbf{x} \in \partial D$, while the stimulus function in D is positive and smooth, at least C^2. Therefore the contour of the work-space is a level set of the stimulus. We consider stimuli as functions $S : D \cup \partial D \to \Re^+ \cup \{0\}$ such that
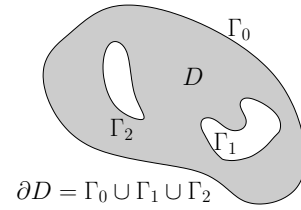

Fig. 2. Domain where the stimulus is defined. The connected domain can be defined as the area enclosed by a set of curves Γ_i, and it must be bounded.

$S(\mathbf{x}) > 0$ iff $\mathbf{x} \in D$. According to [10], there is an increasing connection between the sensors and the motors which we will assume of a functional nature. Therefore, the connection for vehicle 2b can be modelled as an increasing C^2 function $F(s) : \Re^+ \cup \{0\} \to \Re^+ \cup \{0\}$, which means it has a positive derivative, i.e $\frac{dF(s)}{dS} > 0 \forall s \in \Re^+ \cup \{0\}$. Since $F(s)$ represents the turning velocity of each wheel, the vehicle does not move backwards, and we will further assume that $F(0) = 0$, but neither the derivative of $F(s)$ is zero at $s = 0$ nor the gradient of $S(\mathbf{x})$ vanishes at points $\mathbf{x} \in \partial D$. We will denote the Cartesian coordinates of the vehicle as $\mathbf{x} = (x, y)$ and its heading as θ, therefore the state will be $(\mathbf{x}, \theta) = (x, y, \theta)$ and it belongs to $D \cup \partial D \times S^1$, where S^1 represents the unit circle.

Under these assumptions, the state of the differential-drive vehicle 2b immersed in $S(\mathbf{x})$ and with a wheel velocity control $F(s)$ evolves according to the following system of differential equations:

$$\dot{x} = F(S(\mathbf{x})) \cos \theta \tag{1}$$
$$\dot{y} = F(S(\mathbf{x})) \sin \theta \tag{2}$$
$$\dot{\theta} = \frac{\delta}{d} \nabla F(S(\mathbf{x})) \cdot \hat{e}_p \tag{3}$$

where $\nabla F(S(\mathbf{x}))$ is the gradient of the composite function, $\hat{e}_p = [-\sin \theta \cos \theta]^T$ is a unitary vector orthogonal to the vehicle's head direction pointing to its left, δ is the distance between the sensors and d is the wheelbase of the vehicle [16]. To simplify the notation we will write $F(\mathbf{x})$ instead of $F(S(\mathbf{x}))$.

Since the linear velocity of the vehicle is $v = F(\mathbf{x})$, the differential equation governing its acceleration ($\dot{v} = \nabla F(\mathbf{x}) \cdot \dot{\mathbf{x}}$) can be written, using equations (1) and (2), as:

$$\dot{v} = v \nabla F(\mathbf{x}) \cdot \hat{e} \tag{4}$$

where $\hat{e} = [\cos \theta \sin \theta]$ is the unit vector in the heading direction of the vehicle, and we used the fact that $v = F(\mathbf{x})$. On the other hand, assuming $\frac{\delta}{d} = 1$, we can write equation (3) in the more convenient form:

$$\dot{\theta} = \frac{F(\mathbf{x})}{v} \nabla F(\mathbf{x}) \cdot \hat{e} \tag{5}$$

This mathematical model of Braitenberg vehicle 2b allows

us to drive conclusions about its trajectories and select adequate stimulus and connection function to obtain a desired behaviour.

B. Some results on the behaviour of the vehicle

It is worth noting that, given our choices for $S(\mathbf{x})$ and $F(s)$, the dynamical system describing the behaviour of the vehicle has no equilibrium points in D, since equations (1) and (2) never vanish simultaneously.

We will first see that, under the assumptions of section II, the solution of the Cauchy problem (1), (2), (3), $\mathbf{x}_0 \in D$ and $\theta_0 \in (-\pi, \pi]$ stays in D for all t, i.e. $D \times S^1$ is a positive invariant set. Since the right hand side of the dynamical system is continuous, for one solution to go outside the surface of the state space defined by $\partial D \times S^1$, the flow should have a component pointing outside it. By construction of $F(\mathbf{x})$ the first two components of the flow are zero at the boundary, $F(\mathbf{x}) = 0$ for all $\mathbf{x} \in \partial D$, while the normal vector $(\nabla S(\mathbf{x}), 0)$ pointing outside the surface $\partial D \times S^1$ has no angular component. Therefore, the dot product of the flow and the normal vector to $\partial D \times S^1$ is zero. This is because, either the flow is tangent to the surface $\partial D \times S^1$ or it completely vanishes (when equation (3) becomes zero). This result justifies our choice of $F(\mathbf{x})$ to vanish at the boundary ∂D, for the vehicle not to escape from the work-space D.

Another important result about the dynamical system at hand is that no equilibrium point of equations (1), (2) and (3) is stable. Since $F(\mathbf{x})$ only vanishes for $\mathbf{x} \in \partial D$ the only possible equilibria lay at the boundary of D. We assumed that the gradient is not zero at the boundary and, therefore, the only points where the whole flow vanishes are $(\mathbf{x}_0, \theta_0) \in \partial D \times S^1$ such that $\nabla F(\mathbf{x}_0) \cdot \hat{e}_p = 0$, when the vehicle direction coincides with the direction of the gradient of $F(\mathbf{x})$. If we linearise the flow (1), (2) and (3), and compute the Jacobian matrix to perform a linear stability test we get:

$$J(\mathbf{x}_0, \theta_0) = \begin{bmatrix} \nabla F(\mathbf{x}_0)\hat{e}^T & \mathbf{0} \\ \frac{\delta}{d}\nabla F_{x|y}(\mathbf{x}_0)^T \hat{e}_p & -\frac{\delta}{d}\partial_{\hat{e}}F(\mathbf{x}_0) \end{bmatrix} \quad (6)$$

where $\nabla F_{x|y}(\mathbf{x}_0)^T \hat{e}_p$ is a 1×2 row sub-matrix containing the partial derivatives of the gradient w.r.t. x and y, and $\partial_{\hat{e}}F(\mathbf{x}) = \nabla F(\mathbf{x}) \cdot \hat{e}_0$ is the directional derivative of $F(\mathbf{x})$ along the direction of the vehicle $\hat{e}_0 = [\cos\theta_0 \sin\theta_0]^T$. The eigenvalues of the Jacobian matrix indicate the stability of each equilibrium point. These eigenvalues are $\lambda = \left\{0, \nabla F(x_0)\hat{e}_0, -\frac{\delta}{d}\nabla F(x_0)\hat{e}_0\right\}$, and since they have opposite signs one is always positive, which means the equilibrium is a saddle point. The eigenvector corresponding to the zero eigenvalue has the direction orthogonal to the vehicle heading, and therefore accounts for the non-holonomic motion constraints. Since one of the eigenvalues is always negative a one dimensional stable manifold exists for each equilibrium point. However, for a real implementation on a robot this means the equilibrium will never be reached because of the inherent noise on real sensors which drives the trajectory away of the unidimensional stable manifold. Therefore, all the equilibria in the dynamical system describing Braitenberg

vehicle 2b are saddle points. These two results together, D being an positive invariant set and ∂D having only saddle points, imply that the vehicle will never collide with obstacles in the environment, but will move continuously in the work-space. Limit cycles could appear but, finding the limit cycles of non-linear dynamical systems is an open research problem. Some results [16] for circularly symmetric stimulus $S(\mathbf{x}) = S(r)$ indicate that periodic orbits exist but they are not limit cycles.

C. Equivalence with a mass in a potential well

In this section we will prove that the motion equations of a Braitenberg vehicle 2b are equivalent to the motion of a particle in a potential well. Moreover, we will identify the relation between the stimulus function and the potential function. The notion of potential based methods was established long ago in robotics to design controllers [17]. The interesting point in this work is that, despite Braitenberg vehicles being biologically inspired, a mathematical equivalence to a mechanical system can be made. The motion equations in Cartesian coordinates of a friction-less particle of unit mass in a 2D potential well $V(\mathbf{x})$ can be stated as:

$$\dot{\mathbf{x}} = \mathbf{v} \quad (7)$$
$$\dot{\mathbf{v}} = -\nabla V(\mathbf{x}) \quad (8)$$

where $\mathbf{x} \in \Re^2$ and $\mathbf{v} \in \Re^2$ are, respectively, the position and velocity of the particle. These equations can be easily derived using, for instance, Lagrangian mechanics. For this system, instead of Cartesian coordinates, the velocity can be expressed as its modulus (v) and direction (ψ), and their relation to the Cartesian velocities is given by $\mathbf{v} = v\hat{\mathbf{u}}$ where $\hat{\mathbf{u}} = (\cos\psi \sin\psi)^T$. If we express equations (7) and (8) in terms of v and ψ using the coordinate transform, i.e. substituting $\mathbf{v} = v\hat{\mathbf{u}}$ into (7) and (8) and multiplying by the inverse Jacobian of the transformation, we obtain:

$$\dot{\mathbf{x}} = v\hat{\mathbf{u}} \quad (9)$$
$$\dot{v} = -\nabla V(\mathbf{x}) \cdot \hat{\mathbf{u}} \quad (10)$$
$$\dot{\psi} = -\frac{1}{v}\nabla V(\mathbf{x}) \cdot \hat{\mathbf{u}}_p \quad (11)$$

where $\hat{u}_p = [-\sin\theta \cos\theta]^T$ is an unit vector orthogonal to $\hat{u}$. If we write the potential function as $V(\mathbf{x}) = -\frac{1}{2}[F(\mathbf{x})]^2$, equations (9), (10) and (11) turn into:

$$\dot{\mathbf{x}} = v\hat{\mathbf{u}} \quad (12)$$
$$\dot{v} = F(\mathbf{x})\nabla F(\mathbf{x}) \cdot \hat{\mathbf{u}} \quad (13)$$
$$\dot{\psi} = -\frac{F(\mathbf{x})}{v}\nabla F(\mathbf{x}) \cdot \hat{\mathbf{u}}_p \quad (14)$$

which are equivalent equations to those of the Braitenberg vehicle with $\frac{\delta}{d} = 1$. Therefore, the motion of a Braitenberg vehicle 2b corresponds to the motion of a particle in a potential well with potential function $V(\mathbf{x}) = -\frac{1}{2}[F(\mathbf{x})]^2$. This has strong implications since it means that all the known

results about the motion of a particle in a potential well also apply to the motion of a Braitenberg vehicle. We will illustrate this in the experimental section III. It can be shown, for instance, that a scalar defining the total energy can be defined for the Braitenberg vehicle, and it remains constant over time. It also applies the fact that for some potential well or stimulus function, the motion of the vehicle could be chaotic, but for simpler potentials (like a parabolic function) chaos does not appear. Everything depends on the selection of $F(\mathbf{x})$; chaotic or non-chaotic behaviour can appear as a function of a parameter selection. This implies that the trajectory of a vehicle will be dense and arbitrarily close to any point on the work-space.

III. A PRACTICAL IMPLEMENTATION FOR MOBILE ROBOTS

We want to apply the theoretical results obtained to a dual drive mobile robot. It seems reasonable that the domain where the vehicle will move has to be the free space. This free space should be bounded, and we want the objects, and the boundary of the space, to define the boundaries of the work-space itself, i.e. ∂D, where $F(\mathbf{x})$ will vanish. One possibility to define a scalar stimulus function $S(\mathbf{x})$ that vanishes at the boundary of the obstacles is selecting the distance to the closest obstacle. However, this is not a good choice since it is only a C^0 function, the derivative will be discontinuous at the points where the distance to two objects is the same (i.e. on the Voronoi diagram). The effect of this is a discontinuity on the right hand side of equation (3), which will only affect the turning rate.

More appropriate ideas to define $S(\mathbf{x})$ functions can be found in the literature [18], like an estimate of the free area around the robot. Figure 3 shows the area a point robot would perceive with a range limited (r_M) proximity sensor (like a laser range scanner). The free area could be computed through a local map from the intersection of the circle around the robot and the obstacles. To keep the computation simpler, we will instead use the free area perceived by the vehicle which can be directly obtained from the sensor readings. It has been shown that the area of overlapping translating polygons is a continuous quadratic polynomial of the translation [19], and so it will be the free area. Moreover, since one of our polygons is a circle the overlapping area and and the free area will be smoother as a function of the robot position. As it can be seen in the figure, when the robot touches the obstacle, the perceived free area drops to half the size of the perceptual circle. We can define a stimulus function as the perceived area minus half of the area in the perceptual circle. This function becomes zero at the boundary of obstacles and is smooth enough to generate a continuous equation (3).

Using the perceived free area to implement a Braitenberg vehicle on a robot would require two proximity sensors covering $360°$ around the robot. As our robots do not posses such sensors, but a single laser scanner mounted on the front of the robot, we approximated the perceived free area by the free area on each half of the readings of the laser scanner.

(a) Perceived free area with a close obstacle. (b) Perceived free area at the boundary of the free space.
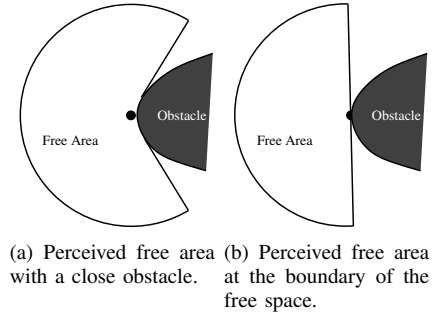
Fig. 3. Definition of the stimulus function $S(\mathbf{x})$ based on the free space perceived by the robot.

Therefore, the laser scan was split into readings from left and right sides, and the area of each side was computed with the corresponding set. Since the robot is not a point, we applied the Minkowski sum of the robot turning radius to the laser scan to obtain the region where the robot is allowed to move. An interesting side effect of using the Minkowski sum is that obstacles with sharp edges become smooth, and thus the function $S(\mathbf{x})$ becomes smoother. In this case, we select the $F(s)$ to be a linear function of the normalised area between zero and the maximum speed of the robot v_M.

Lastly, robots have hardware limitations, and they cannot reach arbitrarily low speeds, needed when the robot is close to obstacles. To overcome this implementation problem, we identified the minimum reachable linear (v_m) and angular (ω_m) velocities and set the turning speed $\omega = sign(\omega) \cdot \omega_m$ when both velocities were below these thresholds. The experiments presented in the rest of this section were performed using a MetraLab SCITOS G5 robot in a square environment of 5.3 m side bounded by a fence. Accurate position information of the robot was obtained from a VICON tracking system mounted around the arena.

A. Simple Environment

This section illustrates the non chaotic behaviour of the Braitenberg vehicle controlled by the perceived free area. For the mass in the potential well, non chaotic behaviour appears for instance in a smooth symmetric potential. We designed the environment to be symmetric, as shown in figure 4, with a square obstacle approximately in the centre of the arena. The sides of the obstacle were parallel to the fence and the robot run 27 laps around it. The trajectory of the robot is also shown in figure 4 with the starting position marked as $\mathbf{x}$ (though the correspondence of the trajectory and the environment in the figure is approximate). The vehicle turns continuously around the obstacle always in the same direction, which depends on its initial pose. This behaviour clearly compares to a particle in a potential well since, for the symmetric case, the turning direction is determined by the direction of the initial velocity. Periodic trajectories appear in this situation, but if the particle velocity is not properly aligned it will oscillate around them. The existence of periodic and quasi-periodic trajectories with two frequencies, has been identified theoretically for symmetric
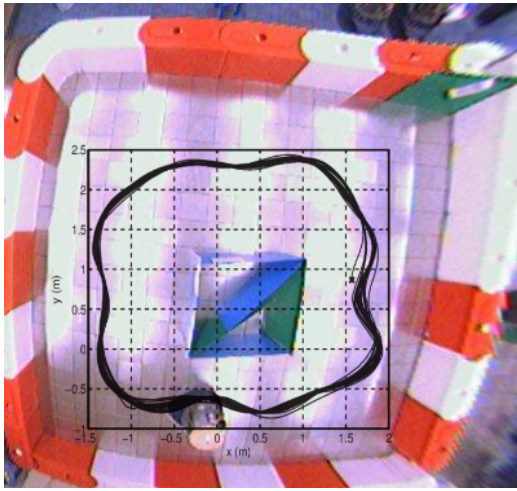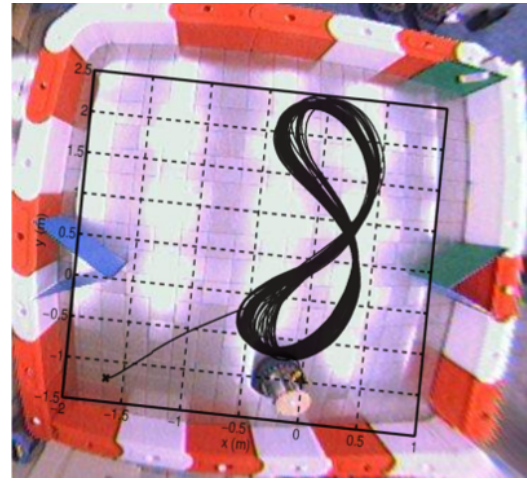
Fig. 4.   Experiment with a symmetric stimulus.

(a) Trajectory of the Braitenberg vehicle in a environment generating a double peaked $S(\mathbf{x})$

(b) Chaotic trajectory of the Braitenberg vehicle

Fig. 5.   Experiments with a double peaked stimulus.

stimuli in Braitenberg vehicle 2b [16]. This experiment confirms these trajectories also appear on implementations in real robots. This is a very special setting, since most of the environments where mobile robots move do not present such a strong symmetry.

B. Double potential well

In this experiment, as figure 5(a) shows, we created a free area stimulus function with two peaks. Two objects were placed on the middle of opposite sides of the arena, therefore the perceived free area will have two maxima at the centre of each of the sides and a local minimum between these obstacles. Figure 5(a) also shows the trajectory of the robot under these conditions, where **x** indicates its starting position. As the figure shows the variability on the trajectory increases with respect to the one presented in figure 4, but it does not display clear sings of chaotic behaviour. On the other hand, this trajectory can be also understood in terms of the mass in a double potential well analogy, as the particle will cycle around both potential valleys and the velocity at the intersection point will have different directions.

Chaotic behaviour is obtained in dynamical systems for some parameter ranges. In our case if the shape of the potential well is changed. One option is to make the potential flat on some regions making a particle behave as a billiard ball on a pool table (where the potential is flat and infinity at the border). It is well know that ideal systems (friction-less with elastic collisions) like billiard balls behave chaotically [20] on these flat potentials (billiard tables). In the case of the perceived free area this can be achieved by simply cutting off the range of the laser scanner, making the robot blind to far obstacles. This generates areas in the environment where the perceived free area is constant and, therefore, the robot will follow a straight line, like a particle moving on a horizontal flat surface. Once an object enters the perceptual range, the speed of the robot will decrease and it will start turning, like a particle climbing a smooth slope. The corresponding experiment is shown in figure 5(b), where the "nearsighted"
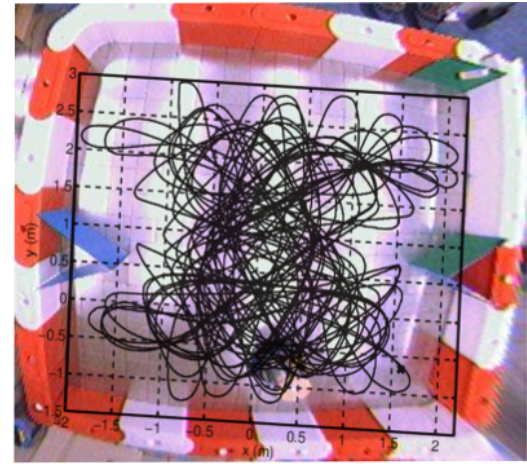
robot ran for more than 30 min in the double peaked flat stimulus. The trajectory shows no clear pattern, it looks random but it is generated by a deterministic controller in a static environment. In the ideal case of a completely planar stimulus with an zero value at the contour of the obstacles the velocity component orthogonal to the surface would change its direction, like a ball hitting the side of a pool table.

C. Complex environments

Our final experiment illustrates the behaviour of the robot on the same arena with four obstacles placed in a non symmetric way. Figure 6 shows the environment and the trajectory followed by the robot during the run. As it can be deduced from the trajectory the robot does not hit any of the obstacles or the fence around the arena. The trajectory "bounces" chaotically at the ends of the perceived free space, and its velocity is higher in the less cluttered areas. Like in the previous experiment, some areas are more often visited than others, and when the passage is narrow (relative to the robot turning radius) the trajectory followed maximises the
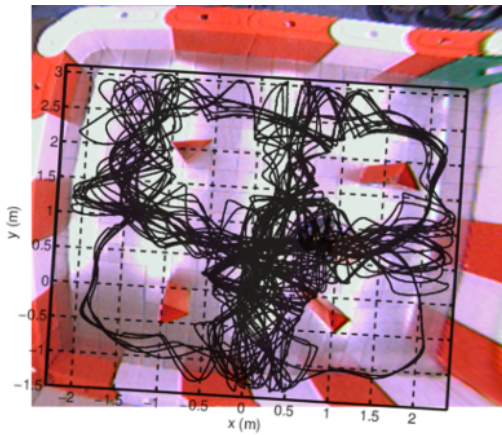
Fig. 6. Experiments in an environment with four obstacles.

distance to the obstacles on both sides.

IV. CONCLUSIONS AND FURTHER WORK

Previous works in chaotic behaviour of robots fall in two categories: they sought chaos on an experimental basis or used chaotic systems to directly control the robot motion. This paper presents the first proof of chaotic behaviour in robotics by showing the equivalence between the equations of Braitenberg vehicle 2b and those of a friction-less mass in a potential well. We identified the relation between the stimulus of the vehicle and the potential function, a powerful analogy which allows to understand how these vehicles behave for a given stimulus. Grounded on the theoretical model of Braitenberg vehicle 2b, we build a stimulus function based on the perceived free area around the robot, that ensures collision free continuous motion within a bounded environment. The trajectories of this controller, in the general case, will be chaotic, and therefore suitable for coverage, exploration or surveillance. This work creates a window of opportunity to apply control of chaos techniques to robotic systems, where the trajectory is filtered through a stable system to attenuate the unstable behaviour and the sensitivity to initial conditions.

A limitation of the proposed implementation is the stimulus function, the perceived free area. Since half of the area the robot can sense is subtracted from the actual free area the motion will be too "conservative" if obstacles appear on opposite sides of the vehicle. This means the speed of the vehicle will be slower than necessary. It will also avoid concave parts of objects since the perceived free area quickly falls to zero. A solution for this problem would consist on building the stimulus function based on the shortest distance to obstacles, at the cost of introducing discontinuities on the turning rate of the robot. A similar problem can occur in potential field approaches when the vehicle enters the area of influence of an obstacle. An alternative would be to define the stimulus as the solution of a partial differential equation with boundary conditions zero at the obstacles, but this would increase dramatically the computational requirements.

Future work includes refining the perceived free area to provide the robot with a less conservative behaviour while keeping the stimulus smooth enough and to investigate the effect of the parameters on the behaviour of the robot in the environment. This would allow to design very simple controllers for coverage, exploration. . .

REFERENCES

[1] L. Kocarev, *IEEE Circuits and Systems Magazine*, vol. 1, no. 3, pp. 6–21, 2001.
[2] K. Cuomo, A. Oppenheim, and S. Strogatz, "Synchronization of lorenz-based chaotic circuits with applications to communications," *IEEE Trans. onCircuits and Systems II: Analog and Digital Signal Processing*, vol. 40, no. 10, 1993.
[3] A. Fradknow and R. Evans, "Control of chaos: survey 1997-2000," in *Proc. of the 32nd IEEE Conf. on Decision and Control*, vol. 1, 1993, pp. 469–474.
[4] Y. Nakamura and A. Sekiguchi, "The chaotic mobile robot," *IEEE Transactions on Robotics and Automation*, vol. 17, no. 6, pp. 898–904, 2001.
[5] C. Volos, I. Kyprianidis, and I. Stouboulos, "A chaotic path planning generator for autonomous mobile robots," *Robotics and Autonomous Systems*, vol. 60, pp. 651–656, 2012.
[6] T. Smithers, "On quantitative performance measures of robot behaviour," *Robotics and Autonomous Systems*, 1995.
[7] U. Nehmzow and K. Walker, "The behaviour of a mobile robot is chaotic," *AISB journal*, vol. 1, no. 4, 2003.
[8] M. Islama and K. Murase, "Chaotic dynamics of a behavior-based miniature mobile robot: effects of environment and control structure," *Neural Networks*, vol. 18, no. 2, p. 123144, 2005.
[9] G. Fraenkel and D. Gunn, *The orientation of animals. Kineses, taxes and compass reactions*. Dover publications, 1961.
[10] V. Braitenberg, *Vehicles. Experiments in synthetic psycology*. The MIT Press, 1984.
[11] E. Bicho and G. Schöner, "The dynamic approach to autonomous robotics demonstrated on a low-level vehicle platform," *Robotics and Autonomous Systems*, vol. 21, pp. 23–35, 1997.
[12] X. Yang, R. V. Patel, and M. Moallem, "A Fuzzy-Braitenberg Navigation Strategy for Differential Drive Mobile Robots," *Journal of Intelligent Robotic Systems*, vol. 47, pp. 101–124, 2006.
[13] T. Salumäe, I. Rañó, O. Akanyeti, and M. Kruusmaa, "Against the flow: A braitenberg controller for a fish robot," in *Proceedings of the International Conference on Robotics and Automation (ICRA)*, 2012, pp. 4210–4215.
[14] V. Lebastard, F. Boyer, C. Chevallereau, and N. Servagent, "Underwater electro-naviagation in the dark," in *Proceedings of the International Conference on Robotics and Automation (ICRA)*, 2012, pp. 1155–1160.
[15] T. Mullin, Ed., *The nature of chaos*. Oxford university press, 1993.
[16] I. Rañó, "A systematic analysis of the braitenberg vehicle 2b for point like stimulus sources," *Bioinspiration & Biomimetics*, vol. 7, no. 3, 2012.
[17] O. Khatib, "Real-time obstacle avoidance for manipulators and mobile robots," *International Journal of Robotics Research*, vol. 5, no. 1, 1986.
[18] I. Rañó and T. Smithers, "Obstacle avoidance through Braitenberg's aggression behavior and motor fusion," in *Proc. of the 2nd European Conf. on Mobile Robots*, 2005, pp. 98–103.
[19] D. Mount, R. Silverman, and A. Wu, "On the area of overlap of translated polygons," *Computer Vision and Image Understanding archive*, vol. 64, pp. 53–61, 1996.
[20] S. Tabachnikov, *Geometry and Billiards*. American Mathematical Society, 2005.